
Article:
Ali, F., Aute, S., Sreedharan, S. et al. (5 more authors) (2018) Tracking HOCl concentrations across cellular organelles in real time using a super resolution microscopy probe. Chemical Communications, 54 (15). pp. 1849-1852. ISSN 1359-7345

https://doi.org/10.1039/c7cc09433g

Journal Name

COMMUNICATION

Tracking HOCl Concentrations Across Cellular Organelles in Real time using a Super resolution Microscopy Probe

Received 00th January 20xx,
Accepted 00th January 20xx

DOI: 10.1039/x0xx00000x

www.rsc.org/

Firoj Ali,[a#] Sunil Aute,[a#] Sreejesh Sreedharan,[b#] Anila H. A,[a] Hiwa K Saeed,[b] Carl G. Smythe,[c*] Jim A. Thomas[b*] and Amitava Das[a,d*c]

BODIPY derivative, SF-1, exclusively shows a fluorescence ON response to HOCl and images endogenously generated HOCl in RAW 264.7 macrophages. Widefield and super resolution structured illumination microscopy images confirm localization in the Golgi complex and lysosomes, and hence specifically detects HOCl generated in these organelles. SF-1 is compatible with 3D-SIM imaging of individual cells.

Bio-imaging technologies to probe the molecular basis of life are in demand. In this context, optical microscopy has proven utility and versatility. Luminescent probes for specific biomolecules and cellular structures are particularly attractive as they provide increased contrast over traditional techniques. The ideal characteristics of cell-permeable probes are that they display low toxicity, organelle specificity, and are photostable with a bright emission. However, one of the disadvantages of conventional fluorescence microscopy is spatial resolution. Even for high-resolution methods, such as confocal laser scanning microscopy (CLSM), two close points appear to merge into one at roughly half the wavelength of the imaging light, restricting resolution to features above ~250 nm. More recently super-resolution microscopy, SRM, techniques that break these limitations have been developed.[1] A case in point is structured illumination microscopy, SIM.[2] Although this form of SRM provides lower resolutions (100 - 120 nm) than STORM and STED - where scaling down to <50 nm has been accomplished - it is a better candidate for live cell imaging as it requires an order of magnitude lower light intensity.[2c]

Optical microscopy has been used to investigate cellular processes, such as the generation of - and cellular response to - reactive oxygen species, ROS. ROS are involved in a range of m cell signaling and regulation processes and dysfunctions that lead to degenerative diseases and cancers

A panoply of processes involved in homeostasis and cell activation is controlled by regulation of the concentration and location of specific ROS. HOCl is an important ROS, which is naturally produced by the myeloperoxidase-H_2O_2-Cl^- system.[3a,3b] This species is catabolized through oxidation by glutathione and cellular thiols and plays a key role in cell death signaling.[3] Thus, detection of HOCl signaling, will plays a key role in understanding the intricacies of these complicated biological mechanisms.

HOCl also plays an important role in the immune response to pathogens,[4] as it is generated during phagocytosis.[5] Activated phagocytic cells generate HOCl[6] as part of the inflammation response. Its overproduction is associated with cardiovascular disease, a neurodegenerative disorder, and inflammatory-related diseases.[7] These effects may be due to quite specific cellular mechanisms; for example, it is suggested that HOCl plays a part in the Golgi stress response, a phenomenon linked to a number of neurodegenerative diseases.[8] However, the role of the Golgi apparatus in HOCl induced oxidative stress is still unclear due to lack of suitable probes. To fully understand such signaling processes, dedicated HOCl probes that display localization in specific cellular compartments are urgently required.[9]

The synthesis of **SF-1** is outlined in Figure 1A. The details of this method, as well as routine analytical and spectroscopic data is provided in the supporting information. The absorption spectrum of **SF-1**, recorded in an aqueous PBS buffer-acetonitrile (9:1, v/v) solution, shows an intense absorption band with a maximum at ~ 550 nm (ε = 40000 L $mol^{-1}cm^{-1}$) and this was assigned to S_0-S_1 electronic transition.[10] On excitation at 550 nm, a weak emission band ($\Phi^{SF\text{-}1}_{586nm}$ = 0.0034) with a maximum at 586nm is observed - Figure 1B.

[a,a] *Organic Chemistry Division, CSIR-National Chemical Laboratory, Pune-411008, India.*
[b] *Department of Chemistry, University of Sheffield, Sheffield, S3 7HF, UK, Email: james.thomas@sheffield.ac.uk*
[c] *Department of Biomedical Science, University of Sheffield, Sheffield, S10 2TN, UK, Email: c.g.w.smythe@sheffield.ac.uk*
[d] *CSIR-Central Salt & Marine Chemicals Research Institute, Bhavnagar: 364002, Gujarat, India; E-Mail: a.das@csmcri.res.in.*
[#] These authors contributed equally to this work.
Electronic Supplementary Information (ESI) available: [Details of synthesis, imaging studies]. See DOI: 10.1039/x0xx00000x

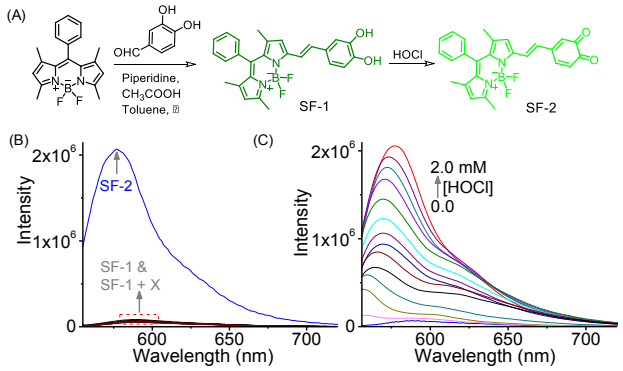

Figure 1. (A) Methodologies adopted for synthesis of **SF-1**; (B) change in emission spectra of **SF-1** in the absence and presence of different ROS/NOS species (HOCl, X: H_2O_2, ·OH, Na_2S_2, HNO, Tyrosinase, Cysteine, NO_3^-, NO_2^-, Fe^{2+}, Fe^{3+}, Cu^{2+}, Cr^{3+}, Hg^{2+}, Zn^{2+} and K^+); (C) emission titration profile for **SF-1** in the presence of varying concentration of HOCl; All emission spectra were recorded using λ_{Ex} = 550 nm in aq. PBS buffer-acetonitrile (9:1, v/v) solution.

A facile charge-transfer process and a low HOMO-LUMO energy gap presumably accounts for its poor emission quantum yield.

The luminescence spectral response of probe **SF-1** towards a variety of species was tested using 20 mole equivalents of the respective analytes. No observable change in luminescence profile was observed in the presence of all other analyte (e.g., X: H2O2, •OH, HNO, Na2S2, NO3$^-$, NO2$^-$, Fe2+, Fe3+, Cu2+, Cr3+, Hg2+, Zn2+ and K+) except for HOCl. On treatment with HOCl, a distinctive "turn-on" luminescence enhancement (Figure 1(B)) with a maximum at 586 nm (Φ^{SF-2}_{586nm} = 0.116; λEx = 550 nm, with Rhodamine B used to evaluate relative emission quantum yield). Even with large excesses of other ROS/RNS and intracellular enzymes like tryosinase, the emission response of SF-1 remains unchanged, illustrating its specificity towards HOCl (ESI†). The lowest detection limit was evaluated using 3σ method to be 4.3 nM in aq. PBS buffer-acetonitrile (9:1, v/v) solution (ESI†). Further studies confirmed that SF-1 was stable across a wide pH range (pH = 4–9) (ESI†). Time-dependent luminescence assays employing 10 μM solutions of the probe in the presence of 2 mM HOCl, reveal that the reaction is completed within 15 min. The HRMS data clearly indicate that reagent **SF-**1 reacts with HOCl to produce SF-2. The higher emission quantum yield for **SF-2** is attributed to an interrupted CT process and enhanced HOMO-LUMO energy gap.[11]

As MTT assays confirmed that both SF-1 and SF-2 are non-toxic towards RAW 264.7 macrophage cells, live cell experiments using wide-field fluorescence microscopy were carried out in which HOCl was added to cells that were previously treated with SF-1. On gradual addition of HOCl, bright wide-field images were observed (ESI). As the probe shows significant emission enhancement in the presence of HOCl and it is chemically robust, we investigated its use in SIM imaging, which requires a bright, highly photostable probe.

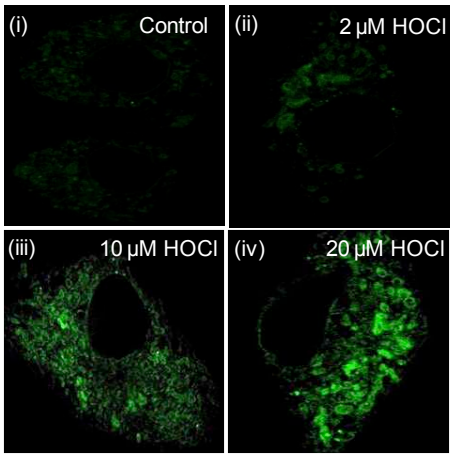

Figure 2. Detection of HOCl by **SF-1**: (i) SIM images of RAW 264.7 cells incubated with SF-1 (10 μM) as the control: (ii–iv) SIM images of cells incubated with **SF-1** (10 μM) for 30 min and then further exposed to different HOCl for 20 min.

To determine the precise localization of SF-1 on interaction with HOCl, experiments were carried out using fixed cells. These experiments confirmed that the probe was compatible with the prolonged irradiation required for SIM, resulting in the images shown in Figure. 2.12,13

After confirming the efficient cellular internalization of the probe and its use in SIM, experiments were performed to map intracellular HOCl, either added externally or endogenously generated by a biochemical process. 3D-SIM images produced during these procedures - processed using Image J - showed a distinctive pattern of localization within the cytosol (see ESI for Images and ESI video 1 of these experiments).

As expected, RAW 264.7 cells treated with only SF-1 (10 μM) showed minimal intracellular fluorescence. However, cells exposed to increasing concentrations of HOCl show a concomitant increase in SF-1 emission. These promising results prompted us to look at imaging endogenously generated HOCl. As RAW cells generate HOCl when they are stimulated by lipopolysaccharide (LPS),14 cells were incubated with LPS (5000 ng/mL) for 12 h in DMEM culture medium with 10% FBS and then further treated with SF-1 (10 μM) for another 30 min. After employing this protocol, SIM images showed bright fluorescence signal from the cells (Figure 3).

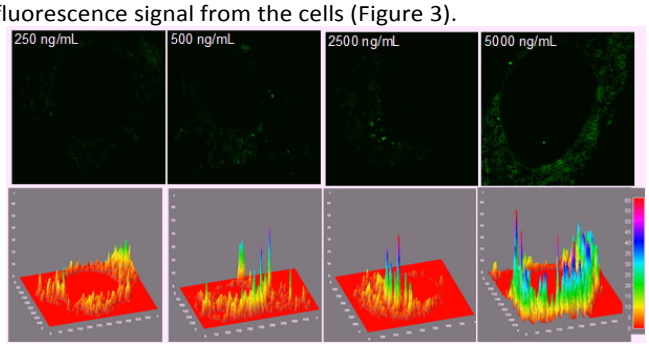

Figure 3. Detection of Endogenous HOCl by **SF-1**: SIM images and emission intensity profiles of **SF-1** in the presence of different concentration of LPS incubated for 12h in fixed RAW 264.7 cells.

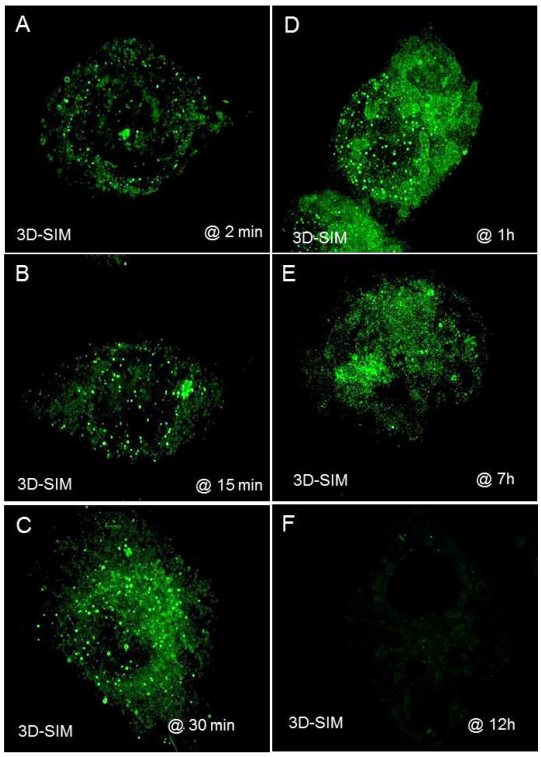

Figure 4. 3D-SIM Images of endogenous HOCl formation and attenuated signal spread generated by LPS stimulation (2500 ng) detected by SF-1 (10 µM). (A) & (B): Signal detection on punctated structures, (B), (C) & (D): Signal spread from puncters to diffuse structures, (E): shows more diffuse structures than puncters indicating total signal transfer to diffuse structures from puncters, (F): Signal saturation due to less availability of endogenous HOCl (indication of cell death).

To understand intracellular bio-signaling mechanisms, it would be advantageous to monitor endogenous signaling spreading across multiple cellular compartments, as this would facilitate a deeper understanding of the signaling pathways between different cellular compartments. Therefore, to trace the fate of HOCl, time-dependent LPS experiments were carried out at a fixed concentration of **SF-1** (10 µM) and LPS (2500 ng) at time intervals ranging from 2 minutes to 12 h and studied by 3D-SIM (Figure. 4).

Emission was initially generated from punctated structures, it then spread out to diffuse through specific areas of the cytosol; indicating that the HOCl is generated, and interacts with SF-1 in certain regions inside the cells, Figure 4. After 12 hours or more, the emission signal dies out completely. The intense signals observed during the initial LPS treatment indicates that HOCl generation is at a maximum during LPS stimulation and then slowly reduces over a period of hours by attenuation through the cytoplasm.

It was evident that **SF-1** does not localize in the nucleus, but is found in specific regions of the cytoplasm. Further details of its exact sub-cellular localization were explored through co-localization experiments

Initial studies involved ER-Tracker as a co-stain. SIM Images from co-staining with **SF-1** (Figure 5A), show low colocalization, with a calculated Pearson's correlation coefficient (PCC) of < 0.05 – see the ESI for scatter correlation diagrams and SI video 2. Contrastingly, colocalization experiments with Cytopainter Golgi Green show a very close spatial correlation between this probe and **SF-1** - Figure 5B. A number of QSAR studies have shown that small molecule localization in specific organelles is highly dependent on the charge and balance of lipophilicity and hydrophilicity of the probe in question.[15] These studies indicate that the low charge/intermediate amphiphilicity of probe **SF-1** lead to Golgi apparatus uptake.

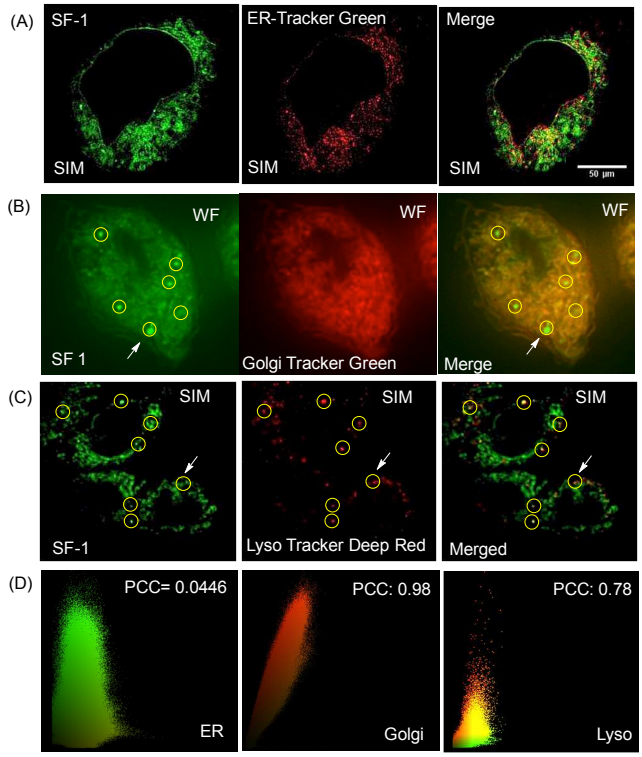

Figure 5. Colocalization experiments (Cells were pre-treated with LPS, 2500 ng before SF-1 and Tracker incubation): (A) SIM images of SF-1, ER-Green and merged indicating minimum colocalization, (B): Wide Field images of SF-1, Golgi Tracker Green and Merged indicating maximum colocalization, (C): SIM images of SF-1, LysoTracker Deep Red and Merged indicating preferential localization of SF-1 to lysosomes, circles showing lysosomes, (D): Comparative Pearson's profile, ER experiment showing minimum colocalization were as Golgi and Lyso experiment showing appreciable colocalization indicating that SF-1 localizes preferentially on Golgi apparatus and Lysosomes.

A calculated Pearson's Coefficient of 0.98 confirmed that **SF-1** detects HOCl within Golgi bodies of cells, See Figure 5B & ESI† (Video-3a and scatter graphs).

Attempts to confirm the localization of **SF-1** within the Golgi body using super resolution imaging proved to be unsuccessful as, due to photobleaching, CytoPainter Golgi Green was not suitable as a SIM probe (See SI Video-3b). Clearly, in this respect, the extraordinary photostability of **SF-1** is superior to this commercial probe and is thus the first SR probe for HOCl in the Golgi apparatus.

To determine the identity of the punctated structures observed during the time-dependent HOCl detection, further colocalization experiments were performed. It was found the emission from **SF-1** co-localised with LysoTracker Deep Red, as confirmed from the generated Pearson's Coefficient values and 3D-SIM images as shown in Figure. 5C, confirming that the punctated structures, and initial source of HOCl, is the lysosome (See SI Video-4). Interestingly treatment with **SF-2,**

freshly generated outside cells, showed an almost identical distrubution, See SI, indicating that HOCl is imaged within this organelle due to th probe's localisation. To understand complex biological processes, it is often necessary to employ more than one probe so that information on simultaneous biological processes can be obtained.[16] Therefore the use of probe **SF-1** in two colour SIM experiments was investigated. For this technique, a organelle probe with different spectral characteristics is required. In this initial study, we used the nuclear stain Hoechst 33442 to yield dual colour SIM images. The high photostability of both probes meant that they could be used to construct striking 3D-SIM images of individual cells – Figure. 6 (see SI for videos).

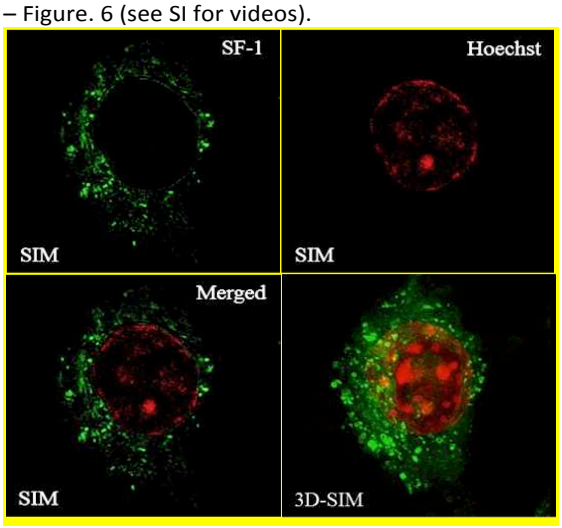

Figure 6: Dual colour SIM and 3D-SIM using **SF-1** in the presence of LPS and Hoechst 33442.

To summarize, a new probe, which detects HOCl, an important ROS molecule generated by macrophages, is reported. The probe localizes in the lysosomes and Golgi complex of live cells and can be used to detect endogenously generated HOCl using SIM, thus providing lateral resolutions of 120 nm. Future studies will use the probe to focus on bio-signaling involving HOCl.

Conflicts of interest

There are no conflicts to declare.

Notes and references

A.D. acknowledges SERB (India) Grants (SB/S1/IC-23/2013 & JCB/2017/000004) for funding. FA, SA and AHA acknowledge CSIR & UGC for their research fellowships. SS and JAT are grateful to the Imaging Life initiative of the University of Sheffield for the studentship to SS and access to the Wolfson Light Microscopy Facility funded by the MRC grant MR/K015753/1. HKS acknowledges KRG scholarship. FA, AD, and JAT are grateful to the GCRF for funding a visit by FA to Sheffield. Finally, we are grateful to the referees, whose constructive comments have greatly improved the quality of this report.

1 (a) M. Baker, *Nature,* 2011, **478**, 137; (b) L. Schermelleh, R. Heintzmann and H. Leonhardt, *J. Cell Biol*., 2010, **190**, 165; (c) C. Eggeling, K. I. Willig, S. J. Sahl and S. W. Hell, *Q. Rev. Biophys*., 2015, **482**, 178.

2 2. (a) L. Shao, P. Kner, E. H. Rego and M. G L. Gustafsson, *Nature Methods,* 2011, **8**, 1044; (b) M. Gustafsson, *Proc. Natl. Acad. Sci. U.S.A,* 2005, **102**, 13081; (c) D. Li, L. Shao, B. C. Chen, X. Zhang, M. Zhang, B. Moses, et al. *Science,* 2015, **349**, aab3500.

3 3. (a) W. M. Nauseef, *Cellular Microbiol*., 2014, **16**, 1146; J. P. Gaut, G. C. Yeh, H. D. Tran, J. Byun, J. P. Henderson, G. M. Richter, M.-L. Brennan, A. J. Lusis, A. Belaaouaj, R. S. Hotchkiss, J. W. Heinecke, *Proc. Natl. Acad. Sci*. 2001, **98**, 11961; (c) J. M. Pullar, M. C. M. Vissers and C. C. Winterbourn, *IUBMB Life,* 2000, **50**, 259.

4 4. S. Kenmoku, Y. Urano, H. Kojima and T. Nagano, *J. Am. Chem. Soc*., 2007, **129**, 7313.

5 5. C. C. Winterbourn, M. B. Hampton, J. H. Livesey and A. J. Kettle, *J. Biol. Chem*., 2006, **281**, 39860.

6 6. Y-ting T. Yang, M. Whiteman and Steven P. Gieseg, *Biochim. Biophys. Acta,* 2012, **1823**, 420.

7 7. (a) Y. W. Yap, M. Whiteman and N. S. Cheung, *Cell Signal,* 2007, **19***,* 219; (b) Q. Xu, K.-A. Lee, S. Lee, K. M. Lee, W.-J. Lee and J. Yoon, *J. Am. Chem. Soc*., 2013*,* **135**, 9944.

8 8. Z. Jiang, Z. Hu, L. Zeng, W. Lu, H. Zhang, T. Li and H. Xiao, *Free Radic Biol Med*., 2011, **50**, 907.

9 9. (a) H. Zhu, J. Fan, J. Wang, H. Muand and X. Peng, *J. Am. Chem. Soc.,* 2014, **136**, 12820; (b) L. Yuan, L. Wang, B. K. Agrawalla, S.-J. Park, H. Zhu, B. Sivaraman, J. Peng, Q.-H. Xu and Y.-T. Chang, *J. Am. Chem. Soc.,* 2015, **137**, 5930; (c) P. Panizzi, M. Nahrendorf, M. Wildgruber, P. Waterman, J.-L. Figueiredo, E. Aikawa, J. McCarthy, R. Weissleder and S. A. Hilderbrand, *J. Am. Chem. Soc*., 2009, **131**, 15739; (d) M. Ren, B. Deng, K. Zhou, X. Kong, J.-Y. Wang, G. Xu and W. Lin, *J. Mater. Chem. B,* 2016, **4**, 4739; (e) H. S. Jung, J. Han, A.-H. Lee, J. H. Lee, J.-M. Choi, H.-S. Kweon, J. H. Han, J.-H. Kim, K. M. Byun, J. H. Jung, C. Kang and J. S. Kim, *J. Am. Chem. Soc*., 2015, **137**, 3017; (f) X. Chen, K. –A. Lee, X. Ren, J.-C. Ryu, G. Kim, J.-H. Ryu, W.-J. Lee and J. Yoon, *Nat. Protoc.,* 2016, **11**, 1219; (g) J. Zhou, L. Li, W. Shi, X. Gao, X. Li and H. Ma, *Chem. Sci*., 2015, **6**, 4884; (h) X. Chen, F. Wang, J. Y. Hyun, T. Wei, J. Qiang, X. Ren, I. Shin and J. Yoon, *Chem. Soc. Rev*., 2016, **45**, 2976; (i) H. Chen, H. Shang, Y. Liu, R. Guo and W. Lin, *Adv. Funct. Mater*., 2016, **26**, 8128.

10 . F. Ali, A. H. A., N. Taye, R. G. Gonnade, S. Chattopadhyay and A. Das, *Chem. Commun*., 2015*,* **51**, 16932.

11 (a) Y. Jiang, G. Zheng, N. Cai, H. Zhang, Y.Tan, M. Huang, Y. He, J. He and H. Sun, *Chem. Commun*., 2017, **53**, 12349; (b) J. Kim and Y. Kim, *Analyst,* 2014, **139**, 2986; (c) W. Zhang, C. Guo, L. Liu, J. Qin and C. Yang, *Org. Biomol. Chem*., 2011, **9**, 5560.

12 Handbook of Biological Confocal Microscopy, third edition, edited by James B. Pawley, *Springer Science and Business Media*, *New York,* **2006**, pp-453.

13 M. G. Gustafsson, *J. Microsc*., 2000, **198**, 82.

14 Y. Adachi, A. L. Kindzelskii, A. R. Petty, J. B. Huang, N. Maeda, S. Yotsumoto, Y. Aratani, N. Ohno and H. R. Petty, *J. Immunol*., 2006, **176**, 5033.

15 R W Horobin, F Rashid-Doubell, J. D. Pediani, G. Milligan, *Biotech. Histochem*., 2013, **88**, 440.

16. P. A. Pellett, X. Sun, T. J. Gould, J. E. Rothman, M. Q. Xu, I. R. Jr. Correa and J. Bewersdorf, *Biomed. Opt. Express,* 2011, **2**, 2364.

